Werk

Jahr: 1975
Kollektion: fid.geo
Signatur: 8 Z NAT 2148:41
Digitalisiert: Niedersächsische Staats- und Universitätsbibliothek Göttingen
Werk Id: PPN1015067948_0041
PURL: http://resolver.sub.uni-goettingen.de/purl?PPN1015067948_0041

LOG Id: LOG_0065
LOG Titel: Supersonic plasma flow between high latitude conjugate ionospheres
LOG Typ: article

Übergeordnetes Werk

Werk Id: PPN1015067948
PURL: http://resolver.sub.uni-goettingen.de/purl?PPN1015067948
OPAC: http://opac.sub.uni-goettingen.de/DB=1/PPN?PPN=1015067948

Contact

Niedersächsische Staats- und Universitätsbibliothek Göttingen
Georg-August-Universität Göttingen
Platz der Göttinger Sieben 1
37073 Göttingen
Germany
Email: gdz@sub.uni-goettingen.de

J. Geophys. 41, 413–439, 1975

Supersonic Plasma Flow between High Latitude Conjugate Ionospheres

G. Rösler

Max-Planck-Institut für Physik und Astrophysik,
Institut für extraterrestrische Physik, Garching bei München

Received October 3, 1974; Revised Version February 3, 1975

Abstract. The polar wind problem has been investigated for closed field lines in situations where one of the two conjugate ionospheric regions is fully illuminated by the sun and the other in darkness (solstices at high latitudes). A supersonic flow between hemispheres is possible; the magnetospheric part of this flow must be symmetric with respect to the equator. The daytime fluxes are proportional to the neutral hydrogen density (n_H). Fluxes of the order of 10^8 cm^{-2} sec^{-1} are only possible with n_H considerably higher than given by CIRA models. For stationary solutions higher flow speeds are needed on the dark side than provided from the illuminated side. It is concluded that shock waves with upward velocities of about 5 km/sec would form above the dark ionosphere. This implies a reduction by a factor of 3 to 5 of the plasma influx into the dark hemisphere, whereby F-layer densities of only up to $2 \cdot 10^4$ cm^{-3} can be maintained.

Key words: Daytime Polar Wind – Free Flow along Field Lines – Supersonic Influx – Non-Stationary Shock Waves.

I. Introduction

The stability of F-layer densities during nighttime when photoionization ceases to act as an ionization source and recombination should reduce the ion densities gave rise to many theoretical and experimental studies during the last ten years. Thermal plasma fluxes from the protonosphere have been suggested rather early as a means of maintaining nighttime F-layers for midlatidude conditions (Rishbeth, 1963; Hanson and Patterson, 1964; Yonezawa, 1965). Fluxes of the order of 10^8 cm^{-2} sec^{-1} turned out to be necessary for stationary F-layers of 10^5 cm^{-3}. Theoretical calculations of the limiting daytime fluxes into the protonosphere indicating maximum fluxes of some 10^7 cm^{-2} sec^{-1} (for example Hanson and Patterson, 1964; Geisler, 1967), however, seemed to restrict this mechanism severely and dynamical processes like upward drifts caused by neutral winds and electric fields (Hanson and Patterson, 1964; King *et al.*, 1967; Kohl *et al.*, 1968; Stubbe, Chandra, 1970) and effects of corpuscular radiation (Torr, Torr, 1970) and atmospheric composition changes (Rüster, 1971) have been favoured. Nevertheless, there is growing evidence from experimental results (Evans, 1965; Park, 1970) as well as from theoretical investigations (Nagy *et al.*, 1968; Banks, Kockarts, 1973; Park, Banks, 1974) (for instance increasing the daytime fluxes by use of more realistic atmospheric models) that the protonosphere can act efficiently as an ionization reservoir for the nighttime ionosphere at least under certain conditions.

The average electron content of a magnetic flux tube at $L = 4$, located within the plasmasphere under quiet geomagnetic conditions, is about $6 \cdot 10^{13}$ electrons/cm^2

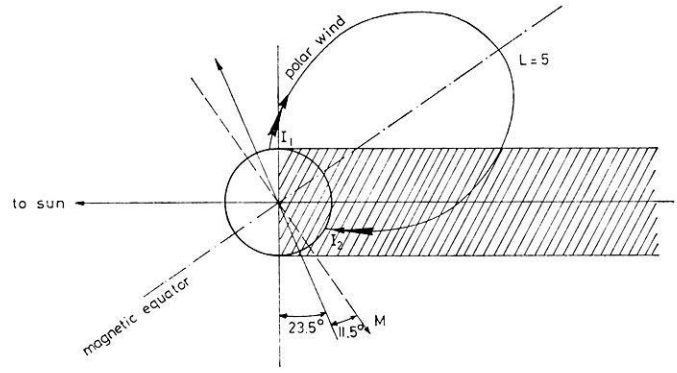

Fig. 1. Asymmetric geomagnetic configuration for solstices and magnetic midnight of the winter ionosphere I_2. The inclination of the rotation axis and the angle between geographic and magnetic axis just add. The summer ionosphere I_1 is still illuminated, the conjugate winter ionosphere I_2 in darkness

tube (e.g. Park, 1970) with an electron density of 10^3—10^4 cm^{-3}. This ionization therefore can supply nighttime fluxes for some days and does not need 'immediate' replenishment. The electron content of a closed flux tube outside the plasmasphere (with n_e of the order of 1 cm^{-3}) at for example $L = 5$—6, however, is at least two orders of magnitude less and cannot maintain downward fluxes of 10^8 cm^{-2} sec^{-1} for several hours unless the loss of ionization is balanced at the same time. Hence concerning high latitude winter conditions influx of plasma along field lines has been discounted because of the lack of a suitable source (Rishbeth, 1970). In this paper a geomagnetic configuration shall be discussed which could allow for such an influx of plasma into the winter nighttime ionosphere by a polar wind from the conjugate summer daytime ionosphere acting as a source of replenishment.

The polar wind problem for closed field lines has been studied for instance in two papers by Mayr, Grebowsky and Taylor in 1970 and by Banks, Nagy and Axford in 1971. In both papers a symmetric configuration corresponding to the magnetic axis perpendicular to the eccliptic plane is assumed with both conjugate ionospheres – which have to be nighttime ionospheres in that case – still emitting polar wind fluxes. By different arguments it is concluded that outward directed polar wind fluxes can be a rather steady phenomenon also for closed flux tubes. In contrast to these investigations of equinotial conditions the field line configuration of this paper corresponding to solstices at high latitudes is a most asymmetric one where the inclination of the magnetic axis is maximum forming an angle of 55° with respect to the eccliptic plane. This situation is shown in Fig. 1. It is evident that in this way a closed field line outside the plasmasphere with an L-value of for example 5 yields a coupling of a summer daytime ionosphere to a winter nighttime ionosphere. Diffusive plasma fluxes as a coupling between two conjugate midlatitude ionospheres have been investigated by Kohl (1966). With respect to high latitude ionospheres topside electron density and ion composition measurements only agree with high speed outward or inward plasma flow. Hence it is our objective to discuss whether a daytime polar wind can represent a mechanism of transport of ionization into the high latitude nighttime ionosphere.

There are two crucial questions connected with this model. The first one is related to the maintenance of outward directed plasma fluxes from the nighttime ionosphere. Without an effective source of ionization recombination and upward flow result in a depletion of ionization. The proton flux at great heights must be supported by an O^+-flux of equal size at lower heights through charge exchange of O^+-ions with neutral hydrogen. (For a review of ionospheric processes see for example Banks, Kockarts, 1973). This O^+-flux is fully developed at a height of about 700 km. With a mean O^+-density of $3 \cdot 10^5$ cm^{-3} and a constant recombination coefficient of $4 \cdot 10^5$ sec^{-1} an O^+-flux of $4 \cdot 10^8$ cm^{-2} sec^{-1} together with recombination would exhaust the ionospheric O^+-reservoir between 200 and 700 km height with a time scale of about 4 hours. This depletion process must be seen in the context of the high latitude convection cycle and the corresponding convection times. According to the work of Dungey (1961), Axford and Hines (1961), Nishida (1966) and Brice (1967) this cycle consists of field line merging at the front of the magnetosphere, convection across the polar caps, reconnection in the tail and migration back towards the sun along the auroral oval. Depending on the L-value of the magnetic flux tube typical convection times range from about four to ten hours. The winter ionosphere I_2 (Fig. 1) spends about three quarters of this cycle in darkness. It is therefore assumed that the nighttime fluxes at least are reduced considerably when both ionospheres I_1 and I_2 are coupled after reconnection. That is, in contrast to the above mentioned papers by Mayr *et al.* (1970) and Banks *et al.* (1971), where two polar wind flows from opposite hemispheres meet at the geomagnetic equator, we adopt for our asymmetric configuration that upward nighttime fluxes are not maintained up to reconnection. As the high latitude exospheric proton density is consistent with outward *and* inward supersonic plasma flow we conclude that the daytime polar wind flux can advance to the nighttime ionosphere at least shortly after reconnection. (It should be emphasized, however, that we do not take into account the effect of particle precipitation in this consideration. Corpuscular ionization may be very important in particular for auroral regions and could cause a much longer time scale for maintaining upward fluxes than derived above.)

The second problem is the effect of reconnection itself on the supersonic daytime fluxes. Preceding reconnection the flux tubes stretch far into the magnetic tail. The mean energy density of the plasma sheet with proton temperatures of the order of some keV, however, is much higher than the critical pressure for polar wind flow which ranges from $5 \cdot 10^{-11}$ to 10^{-10} ergs cm^{-3} (Banks, Holzer, 1969). From a pure hydrodynamic point of view one would expect the formation of shock waves preventing the supersonic flow from reaching the conjugate hemisphere irrespective of whether the nighttime ionosphere is still emitting outward fluxes or not. But clearly a hydrodynamic description is inadequate for this region. At present it appears to be very difficult to assess the effective coupling time between interpenetrating streams of cold and energetic plasmas. No attempt is therefore made to cover this problem and we neglect the presence of energetic particles at high altitudes. Nevertheless, it seems interesting to consider simply a stationary model of the configuration of Fig. 1 based on the assumption that the dominant mechanism in such a flux tube is a polar wind which can flow along closed field lines into a winter nighttime ionosphere. It is the objective of this paper to show the consequences of such a process. In section II the equations and parameters describing ionospheric processes – essentially the same as

used in previous polar wind calculations (Banks, Holzer, 1968, 1969a, 1969b) – are briefly repeated. Section III summarizes some numerical results for daytime conditions. In section IV free flow along field lines is discussed and section V concentrates on the effects of supersonic influx of plasma into the nighttime ionosphere.

II. Hydrodynamic Equations and Parameters

The theory of polar ionospheres has been extensively developed mainly in the papers by Banks and Holzer (Banks, Holzer, 1968, 1969a, 1969b; Banks, 1970, 1971; Holzer, 1970, Holzer *et al.*, 1971). High latitude conditions exhibit for example O^+ remaining the dominant ionospheric constituent up to great heights (some thousand kilometers), much lower electron densities in the topside ionosphere and large scale upward proton fluxes. It has been shown that these special features agree with a model of an expanding ion exosphere. Above F_2-heights photoionization creates an upward O^+-flux which is converted by charge exchange ($O^+ + H \rightarrow H^+ + O$) to a low speed H^+-flux of nearly equal size. Essentially owing to the electron pressure gradient the light ion species, i.e. the protons, is accelerated rather rapidly reaching supersonic speed at altitudes of several thousand kilometers. The coupling between electrons and ions is established by an outward directed polarization field. A great variety of numerical results concerning ion density distributions, escape fluxes and proton velocities for different models has been published in the above mentioned papers. In analogy to solar wind expansion the ionospheric proton flux was termed 'polar wind' as suggested by Axford. The summer daytime ionosphere I_1 (Fig. 1) supplies the boundary conditions of the plasma influx into the winter ionosphere I_2. Therefore, we will deal first with polar wind calculations for the daytime ionosphere only taking account of the appropriate field line configuration and of different atmospheric models.

The equations describing the multi-constituent plasma flow can be written for stationary conditions in the form (Banks, Holzer, 1969b):
Continuity:

$$\frac{1}{A}\frac{\partial}{\partial s}(n_i U_i A) = q_i - l_i \tag{1}$$

Momentum:

$$\begin{aligned}\frac{1}{U_i}\frac{\partial U_i}{\partial s}\left[\frac{U_i^2}{C_i^2} - 1\right] = {} & \frac{1}{C_i^2}\,\mathbf{g}\cdot\mathbf{s} + \frac{1}{A}\frac{\partial A}{\partial s} - \frac{1}{T_i}\frac{\partial T_i}{\partial s} \\ & - \frac{1}{C_i^2}\sum_k \nu_{ik}(U_i - U_k) - \frac{1}{\Phi_i}\frac{\partial \Phi_i}{\partial s} \\ & - \frac{1}{C_i^2 n_e m_i}\frac{\partial P_e}{\partial s} - \frac{q_i}{C_i^2 n_i}U_i\end{aligned} \tag{2}$$

with

$$C_i^2 = kT_i/m_i;\ \Phi_i = n_i U_i A;\ P_{e,i} = n_{e,i}\cdot k\cdot T_{e,i};$$

$n_e = \sum n_i$ and s = coordinate parallel to magnetic field, U = bulk velocity along s, n = number density, A = cross-section of magnetic flux tube, $\mathbf{g} \cdot \mathbf{s}$ = component of gravitational acceleration along s, q_i = ion production rate, l_i = ion loss rate, $T_{i,e}$ = ion, electron temperature, ν_{ik} = momentum transfer collision frequency between i and k type particle, m = particle mass, k = Boltzmann's constant.

The following we will summarize the assumptions and parameters underlying our calculations:

1. Ionospheric Constituents. Only hydrogen and oxygen ions which are the major constituents above F-region heights are considered. The presence of He-ions does not change the results in particular for the proton escape fluxes.

2. Chemical Reactions. With regard to the formation of the F-layer and the ion densities at greater heights ion production and loss is mainly caused by the following reactions (Ferguson, 1967; Mitra, 1968) with the corresponding reaction coefficients λ:

$$O + h\nu \rightarrow O^+, \lambda_1 = 5 \cdot 10^{-7} \text{sec}^{-1}$$

(Banks, Holzer, 1969a)

$$O^+ + N_2 \rightarrow NO^+ + N, \lambda_2 = 5 \cdot 10^{-13} \text{cm}^3\text{sec}^{-1}$$

(Dunkin *et al.*, 1968; Stubbe, 1969)

$$O^+ + O_2 \rightarrow O_2^+ + O, \lambda_3 = 1.6 \cdot 10^{-11} \text{cm}^3\text{sec}^{-1}$$

(Dunkin *et al.*, 1968; Stubbe, 1969)

$$O^+ + H \rightarrow H^+ + O, \lambda_4 = 4.3 \cdot 10^{-11} (T_n + T_i/16)^{1/2} \text{ cm}^3\text{sec}^{-1}$$

(Holzer, Banks, 1969)

$$H^+ + O \rightarrow O^+ + H, \lambda_5 = 3.8 \cdot 10^{-11} (T_i + T_n/16 + 1.2 \cdot 10^{-8} (U(H^+) - U(O))^2)^{1/2} \text{cm}^3\text{sec}^{-1}$$

(Holzer, Banks, 1969)

The molecular ions formed by charge exchange undergo a dissociative recombination reaction according to $AB^+ + e \rightarrow A + B$.

3. Temperatures. For daytime conditions an isothermal model with $T_e = T_i$ is adopted. This assumption may look rather poor as strong positive ion temperature gradients are known to exist between ionospheric levels and for example 3000 km (e.g. Banks, Kockarts, 1973). However, different ion temperature profiles have been inferred by Banks and Holzer (Banks, Holzer, 1969a; Holzer, 1970) in their polar wind studies. It has been shown that the magnitude of the ion temperature is far more important in determining the ion composition profile and the H^+ flow characteristics. The critical solutions (with a continuous transition from supersonic speed to subsonic speed) for the nighttime ionosphere are also calculated under this assumption which is perhaps more severe in that case as the incoming protons are heated by the collisions with the oxygen ions converting translational energy into random thermal energy. Yet these calculations serve only to illustrate the fact that the polar

wind runs into the nighttime ionosphere with a particle density and a mean velocity far from what is required by the critical solutions (see Sect. V). In the discussion of the influx of a realistic polar wind the proton temperature will be considered too.

Neglecting heat conduction the energy balance of the protons can be written as (e.g. Holzer, 1972):

$$\frac{1}{A}\frac{\partial}{\partial s}\left[\Phi_1\left(\frac{1}{2}U_1^2+\frac{\gamma}{\gamma-1}\frac{k\cdot T_1}{m_1}\right)\right]=\mathbf{g}\cdot\mathbf{s}\cdot n_1U_1+\mathcal{Q}_{\mathrm{ce}}+\mathcal{Q}_{\mathrm{coll}} \tag{3}$$

γ = adiabatic constant

(The indices 1 (2) will always refer to the hydrogen (oxygen) ions). The left hand side contains the gradient of the energy flux, the right hand side the influence of gravity and the source terms $\mathcal{Q}_{\mathrm{ce}}$ and $\mathcal{Q}_{\mathrm{coll}}$ describing the energy production per proton mass and unit volume by charge exchange (ce) $H^+ + O \leftrightarrow O^+ + H$ and the collisions (coll) of the protons with the oxygen ions and the neutral atmosphere. The oxygen ions are assumed to have a constant temperature T_i because the energy transfer from the protons is effective only up to altitudes where the O^+-ions are still the major constituent. Because of the high thermal conductivity of the electrons a constant electron temperature is accepted, too.

In the charge exchange process protons are produced which reflect the properties of the O^+-ions (that is $U \approx O$, internal energy $\frac{1}{\gamma-1}kT_i$) and protons with a mean translational energy of $\frac{1}{2}m_1U_1^2$ and internal energy $\frac{1}{\gamma-1}k\cdot T_1$ are lost. The source term $\mathcal{Q}_{\mathrm{ce}}$ therefore is given (in analogy to Holzer, 1972):

$$\mathcal{Q}_{\mathrm{ce}}=q_1\frac{1}{\gamma-1}\frac{kT_i}{m_1}-l_1\left(\frac{1}{2}U_1^2+\frac{1}{\gamma-1}\frac{kT_1}{m_1}\right) \tag{4}$$

where q_1 and l_1 are the respective production and loss rates.

The energy exchange by collisions between the constituents of a multi-component gas mixture has been derived for example by Tanenbaum (1965) from integrating the Boltzmann's equation. One gets:

$$\mathcal{Q}_{\mathrm{coll}}=\sum_i\mathcal{Q}_{\mathrm{coll}}^i$$

$$\mathcal{Q}_{\mathrm{coll}}^i=-n_1\nu'_{1j}\left[\frac{3}{2}\frac{k(T_1-T_i)}{m_1}\cdot\varepsilon-\frac{1}{2}|U_1-U_j|^2\right] \tag{5}$$

The summation extends over all kinds of H^+-collisions. ε depends on the collision cross section and approximates unity for small relative velocities. We adopt this value for all velocities in this paper. The collision frequency for energy transfer ν'_{1j} is connected with the collision frequency for momentum transfer ν_{1j} by:

$$\nu'_{1j}=\frac{2m_1}{m_1+m_j}\cdot\nu_{1j} \tag{6}$$

Eqs. (3) to (5) relate the proton temperature gradient to the velocity derivative and (1) to (5) give a closed set of differential equations for the hydrogen and oxygen ion densities and velocities and the proton temperature which can be solved numerically.

4. Earth Magnetic Field. According to Fig. 1 we consider a magnetic flux tube of a dipole model with an L-value of 5. Clearly a dipole model will be a poor description for closed field lines outside the plasmasphere and an L-value equal to 5 may look rather low for quiet time conditions. The L-value, however, is not decisive for ionospheric problems (for example regarding escape fluxes and escape velocities) where divergence of field lines $\left(\frac{1}{A}\frac{\partial A}{\partial s}\right)$ is not very important. With respect to the magnetospheric part of the polar wind flow the special field line configuration does not affect our results severely. The main point for our discussion is only the existance of a closed field line outside the plasmasphere roughly symmetric to the geomagnetic equator coupling a winter nighttime to a summer daytime ionosphere.

A dipole model yields (with β = geomagnetic latitude, $\xi = \sin\beta$, R_e = earth radius, g_0 = gravitational acceleration at the surface of the earth):

$$ds = R_e L \sqrt{1 + 3\xi^2}\, d\xi \tag{7}$$

$$\frac{1}{A}\frac{\partial A}{\partial S} = 3\xi\left(\frac{2}{1-\xi^2} + \frac{1}{1+3\xi^2}\right) \Big/ (R_e L \sqrt{1+3\xi^2}) \tag{8}$$

$$\mathbf{g}\cdot\mathbf{s} = -g_0 \cdot 2\xi/[L^2(1-\xi^2)\sqrt{1+3\xi^2}] \tag{9}$$

5. Neutral Atmosphere. Models of the neutral atmosphere still seem to involve great uncertainties especially for high latitude regions where continual loss of ionization by polar wind flow also affects the neutral composition (Banks, Kockarts, 1973). In this paper CIRA 1965-models were adopted with mod. 5, $t = 1000$ for daytime and mod. 5, $t = 0$ for nighttime conditions referring to a solar flux of $F = 150 \cdot 10^{-22}$ W/m^{2}c/sec at 10.7 cm wavelength corresponding to a mean solar activity. These models contain a neutral hydrogen density of $n(\mathrm{H}) \approx 9 \cdot 10^3 \mathrm{cm}^{-3}$ at 500 km which is very low compared to the models — especially for low neutral temperatures — used by Banks and Holzer (Banks, Kockarts, 1973). Too low neutral hydrogen densities of CIRA-models have been indicated already by Brace *et al.* (1967) and Mayr *et al.* (1967). To take account of that uncertainty results are also given for increased $n(\mathrm{H})$ in Sect. III and V. The very low proton fluxes yielded by CIRA-models seem to support the suspect that $n(\mathrm{H})_{\mathrm{CIRA}}$ is considerably too low.

6. Collision Frequencies. The collision frequencies for the various constituents are taken from Holzer (1970) and are not repeated here. These collision frequencies result from the geometric mean of the simple asymptotic limits of large and small transport speeds. In the case of the $H^+ - O^+$-collisions this approximation has been compared with the exact value arising from the integration of the Boltzmann's collision integral (Rösler, 1974). For $\nu(H^+) \approx 2 \cdot \sqrt{kT_i/m_1}$ the deviation of both formulas is maximum the actual value exceeding the approximation by about 50%.

Table 1

	neutral hydrogen density $n(H)$	$T_i = T_e$	photoionization rate
mod. I	$n(H)_{CIRA}$	1500 K	$5 \cdot 10 \cdot {}^{7}sec^{-1}$
mod. II	$10 \cdot n(H)_{CIRA}$	1500 K	$5 \cdot 10^{-7}sec^{-1}$
mod. III	$40 \cdot n(H)_{CIRA}$	1500 K	$5 \cdot 10^{-7}sec^{-1}$
mod. IV	$10 \cdot n(H)_{CIRA}$	3000 K	$5 \cdot 10^{-7}sec^{-1}$
mod. V	$40 \cdot n(H)_{CIRA}$	3000 K	$5 \cdot 10^{-7}sec^{-1}$
mod. VI	$10 \cdot n(H)_{CIRA}$	3000 K	$1.67 \cdot 10^{-7}sec^{-1}$

CIRA = CIRA, Mod. 5, $t = 1000$

III. Numerical Results for Daytime Conditions

As mentioned above the principle features of high latitude daytime ionospheres are well known from the polar wind calculations by Banks and Holzer. A brief survey of the rather similar results obtained with the assumptions of Sect. II may, therefore, be sufficient. Characteristics of the different models are listed in Table 1.

A constant photoionization rate of $5 \cdot 10^{-7}sec^{-1}$ may be representative for summer conditions ignoring the effects of optical depth. The winter ionosphere, however, will spend only a few hours at most in sunlight with a zenith angle χ not far from 90°. As shown by Thomas (1966) a change from $\chi = 0$ to $\chi = 90°$ results in a decrease of the corresponding F-maximum densities by a factor 2 to 3. This is equivalent to a reduction of the photoionization rate by the same factor. To illustrate the impact of nearly grazing incidence on the proton fluxes and velocities mod. VI (which has to be compared with mod. IV) therefore takes a lower photoionization rate of one third of the above value.

Evidently Eqs. (1) and (2) contain not only the supersonic solution which implies a unique set of boundary conditions for both ion species at high altitudes but also a variety of subsonic solutions ranging from diffusive equilibrium to a 'first' subsonic solution where the H^+-ions are accelerated to nearly speed of sound at the critical point and then decelerated again at greater heights. Hence this section summarizes numerical results for the different models both for the supersonic solution yielding the maximum proton fluxes and a 'typical' subsonic solution with diffusive H^+-velocities of the order of 100 m/sec.

Two examples of the ion density distributions are shown in Fig. 2 and 3. The profiles indicated by A refer to the subsonic solution, B and C denote the supersonic and the 'first' subsonic solution (as defined above) respectively. With the exception of mod. VI the F-layers are not affected very much by the different models and solutions with O^+-densities of 7—8 $10^5 cm^{-3}$. The lower maximum density of mod. VI is due to the reduced photoionization rate. The subsonic solution is equivalent to a low speed approximation to Eq. (2) which is representative for midlatitude ionospheres. It is characterized by a steady increase in the H^+-density up to a nearly constant value of 10^3—10^4 cm^{-3} at high altitudes according to the large scale height of the protons. On the other hand acceleration to supersonic speed in the polar iono-

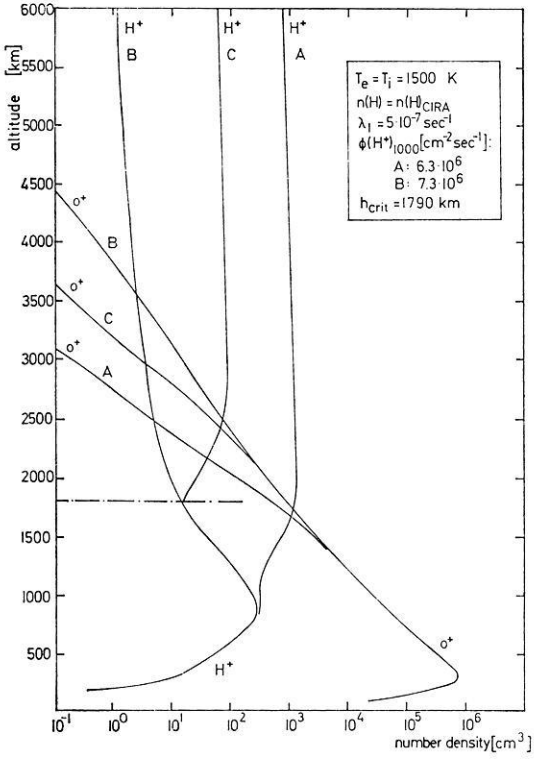

Fig. 2. Daytime ion density profiles for $T_e = T_i = 1500$ K and neutral hydrogen density according to CIRA 1965. A: low speed plasma flow (mid-latitudes), B: supersonic flow (high latitudes); C: 'first' subsonic solution

sphere has the consequence that the proton density reaches a maximum at about 1000 km and decreases after that (see Banks and Holzer). An electron pressure gradient is maintained in this way which is equivalent to an outward directed polarization field and which is mainly responsible for the acceleration of the hydrogen ions. The supersonic and 'first' subsonic profiles are clearly identical up to the critical point. Further decrease in the H^+-density and corresponding acceleration determines the supersonic flow, while an increase in the H^+-partial pressure causes the successive deceleration to lower speeds for the 'first' subsonic solution. The H^+-density range between the profiles A and C can be covered by subsonic solutions with the proton velocity reaching a maximum near the critical point. It is therefore hardly possible (especially for high ion temperature models yielding a less fast H^+-acceleration with the critical point at high altitudes, see Fig. 3) to derive from ion density measurements below the critical point whether supersonic flow really is attained (see Brinton *et al.*, 1971).

In Table 2 we summarize results for the escape fluxes $\Phi(H^+)_{1000}$ (normalized to 1000 km as usual) and the altitudes $h_=$ (defined by $n(H^+) = n(O^+)$) above which the H^+-ions become the major ion species both for the 'typical' subsonic (sb) and the supersonic (sp) solution. The critical heights h_{crit} and the H^+-bulk velocities $v(H^+)_{6000}$ and the corresponding Mach numbers $M(H^+)_{6000}$ at 600 0km height for supersonic flow are also listed there.

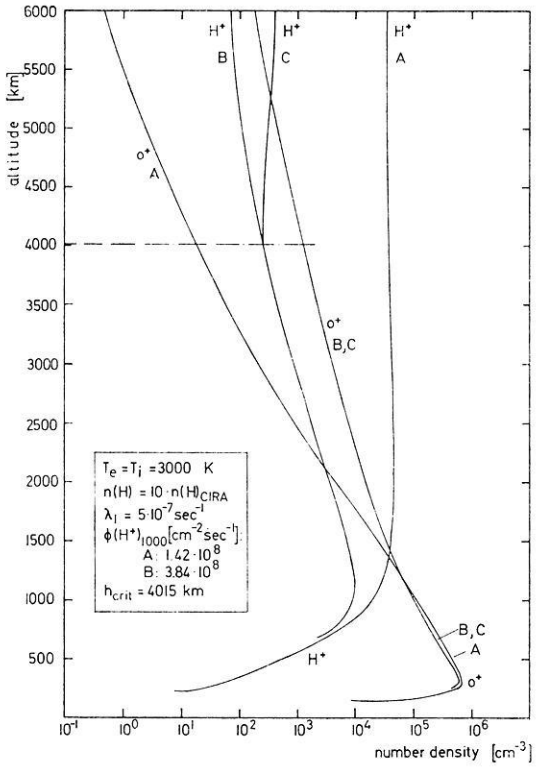

Fig. 3. Daytime ion density profiles for $T_e = T_i = 3000$ K and neutral hydrogen density ten times higher than CIRA 1965. A: low speed plasma flow (mid-latitudes); B: supersonic flow (high latitudes); C: 'first' subsonic solution

Table 2

		$\Phi(H^+)_{1000}$	h_{crit}	$v(H^+)_{6000}$	$M(H^+)_{6000}$	$h_=$
mod. I	(sb)	$6.3 \cdot 10^6$				1680
	(sp)	$7.3 \cdot 10^6$	1790	13.7	3.91	3570
mod. II	(sb)	$5.4 \cdot 10^7$				1320
	(sp)	$7.4 \cdot 10^7$	1900	11.0	3.12	2690
mod. III	(sb)	$1.27 \cdot 10^8$				1040
	(sp)	$2.88 \cdot 10^8$	2250	8.9	2.51	2360
mod. IV	(sb)	$1.42 \cdot 10^8$				1360
	(sp)	$3.84 \cdot 10^8$	4015	11.0	2.19	8400
mod. V	(sb)	$4.0 \cdot 10^8$				1085
	(sp)	$1.05 \cdot 10^9$	5000	7.5	1.51	7795
mod. VI	(sb)	$5.70 \cdot 10^7$				1480
	(sp)	$1.46 \cdot 10^8$	2642	15.0	3.02	6680
		[cm^{-2}sec^{-1}]	[km]	[km/sec]		[km]

Concerning the fluxes two points should be reemphasized: First there is no great difference between the subsonic and supersonic fluxes. That is, polar wind fluxes may be perhaps twice the diffusive midlatitude fluxes and the great discrepancy between the former subsonic calculations of, for example, Hanson and Patterson (1964) and Geisler (1967) and the polar wind fluxes given by Banks and Holzer is mainly caused by different models and not specific to subsonic and supersonic flow. The description of the plasmasphere separating midlatitude and polar ionospheres by Mayr *et al.* (1970) as a region of abrupt change not only in the H^+-density but also in the magnitude of the fluxes along the field line therefore seems doubtful at least at lower heights close to the ionospheres. Secondly, the fluxes are roughly proportional to the neutral hydrogen density (see also Banks, Kockarts, 1973). The CIRA-models with low $n(H)$ yield only fluxes of about $10^7 cm^{-2} sec^{-1}$. Fluxes of the order of $10^8 cm^{-2} sec^{-1}$ which seem to be confirmed both for high- and midlatitudes (Hoffman, 1968, 1971; Park, 1970) require a hydrogen density about ten times higher then given by CIRA. That is another reference to the fact that the neutral hydrogen density of CIRA-models seems considerably too low as stated above. An increase of the ion temperature from 1500 K to 3000 K results in a corresponding increase of the escape fluxes by a factor 4 to 5. A comparison of mod. VI and IV shows the decrease of the proton fluxes caused by a lower photoionization rate indicating that we would expect a lower polar wind flux from a winter daytime ionosphere. It should be noted, however, that this prediction is not verified at all experimentally. Hoffman (1968, 1971) derives maximum polar wind fluxes from satellite measurements for the winter morning hours which cannot be explained by photoionization and stationary models stating the efficiency of other mechanisms like for example corpuscular ionization and heating.

The proton velocity profiles are shown in Fig. 4 and 5. The results agree very well with those of the previous polar wind calculations. A higher ion temperature shifts the critical point to higher altitudes by decreasing the total electron density gradient. An increased neutral hydrogen density also yields a less rapid acceleration and higher critical points. The H^+-escape fluxes, however, are larger for a high density, slowly flowing model than for a low density, rapidly flowing model. This result differs from those of Banks and Holzer (1969). The proton velocities at 6000 km height range from 7 to 14 km/sec, the corresponding Mach numbers from 1.5 to 3.9 (referring to a speed of sound defined by $c(H^+) = \sqrt{kT_i/m(H^+)}$ which amounts to 3,52 km/sec for $T_i = 1500$ K and 4.97 km/sec for $T_i = 3000$ K).

Hence we conclude that the illuminated ionosphere of Fig. 1 will provide supersonic proton fluxes of some $10^8 cm^{-2} sec^{-1}$ with mean velocities reaching Mach numbers of 4 at most at high altitudes which will turn out to be a serious limitation in the discussion of the nighttime ionosphere.

IV. Free Flow along Field Lines

At heights exceeding several thousand kilometers the existence of oxygen ions, collisions and chemical reactions becomes neglegible. The mean velocity of the H^+-plasma is determined then by free flow along the field lines. Below the critical point the mean free path λ for the $H^+ - O^+$-collisions is less or in the order of the O^+-scale height $H(O^+)$ (Banks, Holzer, 1969). The flow therefore can be treated as

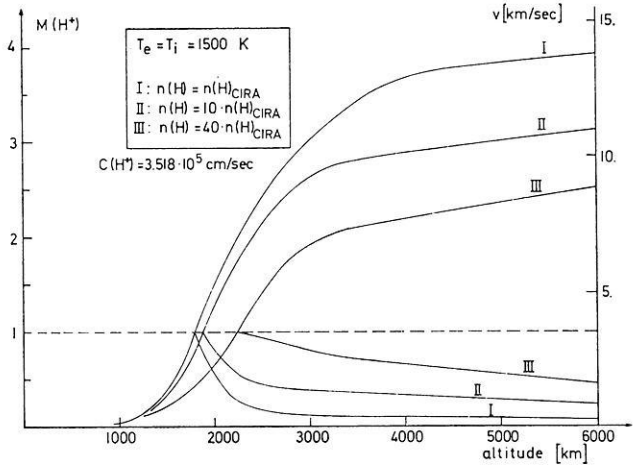

Fig. 4. Proton velocity profiles for supersonic and 'first' subsonic flow for the 1500 K models

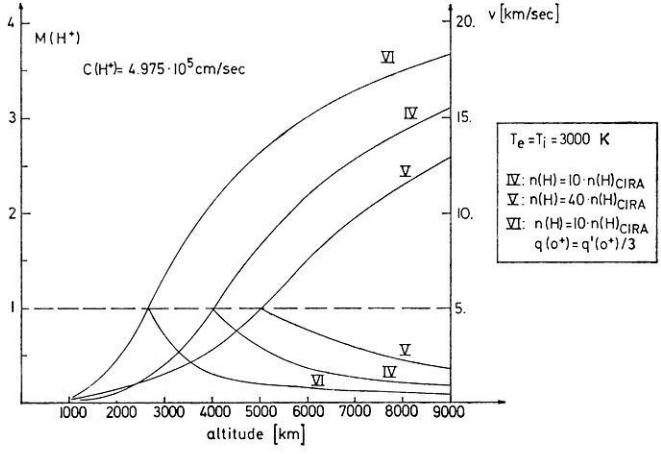

Fig. 5. Proton velocity profiles for supersonic and 'first' subsonic for the 3000 K models

collision dominated ensuring the adequacy of a hydrodynamic description with an isotropic H^+-pressure about the H^+-transport speed. As λ exceeds $H(O^+)$ the flow ceases to be collision dominated and a kinetic description would be appropriate. Decrease of the magnetic field along the flux tube and conservation of magnetic moment of the protons should establish an anisotropic pressure (Banks, Kockarts, 1973). A detailed comparison of kinetic and hydrodynamic models of an expanding ion exosphere by Holzer *et al.* (1971) has shown, however, that the results of both models essentially are the same in the region of supersonic flow. The ion density and velocity distribution is rather insensitive to the form of the proton pressure tensor and hence hydrodynamic equations with an isotropic pressure provide a good description for higher altitudes, too.

The magnetospheric part of the polar wind flow between the two hemispheres therefore is discussed also under this assumption. For isothermal conditions with $T_e = T_i = T$ Eq. (2) for the proton velocity then can be integrated from any point to the magnetic equator (e.g. Parker, 1963):

$$\frac{1}{2}(U^2 - U_e^2) - \frac{2kT}{m}\left[\ln\left(\frac{U}{U_e}\right) + \ln\left(\frac{A}{A_e}\right)\right] + \varphi - \varphi_e = 0 \tag{10}$$

with φ = gravitational potential

(The index i is omitted from now on, the index e refers to the magnetic equator). As pointed out above a dipole model of the geomagnetic configuration is adopted describing a field line by

$$r = R_e \cdot L \cos^2\beta \tag{11}$$

Hence

$$\frac{A}{A_e} = \frac{(1 - \sin^2\beta)^3}{\sqrt{1 + 3\sin^2\beta}} \tag{12}$$

and

$$\varphi = \varphi_e/(1 - \sin^2\beta) \tag{13}$$

While for a multi-constituent plasma the ion Machnumber referred to their speed of sound c_i alone (with $c_i^2 = kT_i/m_i$), an appropriate definition of the proton Machnumber for the single ion species ambipolar Eq. (10) is $M = U/c$ with $c^2 = k(T_i + T_e)/m = 2kT/m$ referring to the speed of sound in the overall proton-electron plasma. Using $\xi = \sin\beta$, $\mathrm{H} = -\varphi_e/c^2$ and (12) and (13) Eq. (10) can be written for the H^+-Machnumber:

$$\frac{1}{2}(M^2 - M_e^2) - \ln\frac{M}{M_e} - \ln\left[\frac{(1 - \xi^2)^3}{\sqrt{1 + 3\xi^2}}\right] + \mathrm{H} - \frac{\mathrm{H}}{1 - \xi^2} = 0 \tag{14}$$

The general pattern of the solutions of Eq. (14) is plotted in Fig. 6 for different values of H. This parameter represents essentially the gravitational potential of the protons at the geomagnetic equator in terms of their mean thermal energy. $\mathrm{H} = 4.5$ separates two different regimes: 1) For $\mathrm{H} > 4.5$ one asymmetric supersonic solution exists reaching the speed of sound at the geomagnetic equator with $\partial M/\partial\xi > 0$ at $\xi = 0$ corresponding to continuing acceleration. 2) For $\mathrm{H} < 4.5$ both kinds of solutions are symmetric to the geomagnetic equator. The critical point for the supersonic solutions is situated at $\xi \neq 0$, the protons are accelerated to maximum speed at the equator with successive deceleration. The subsonic velocity distribution is characterized by a small maximum at the critical height with very low equatorial velocities.

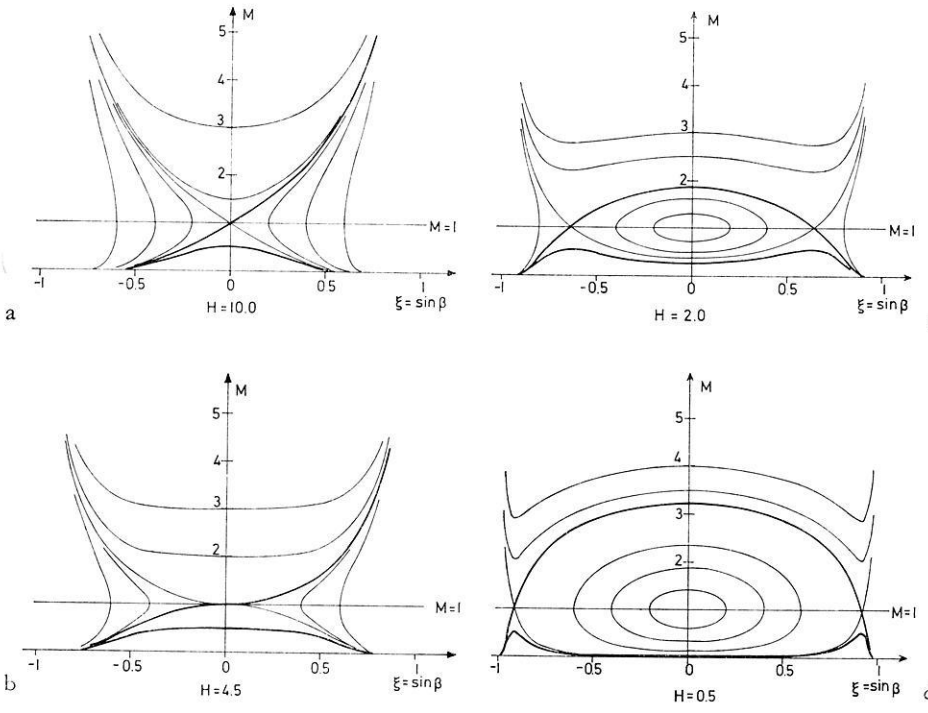

Fig. 6. Solution pattern of the H^+-Mach number as a function of geomagnetic latitude for isothermal free flow conditions. (H denotes the gravitational potential at the magnetic equator in terms of the mean thermal proton energy; $H=0.5$ for $T_i=1500$ K and $L=5$)

With $\varphi_e=-\gamma M/R_eL$ ($\gamma=$gravitational constant, $M=$mass of earth, $R_e=$earth radius) one gets:

$$H=-\varphi_e\Big/\left(\frac{2kT}{m}\right)=\frac{3.8\cdot 10^3}{L\cdot T} \tag{15}$$

An L-value of 5 and a proton temperature of 1500 K yield $H=0.5$. The solutions for that case are shown in Fig. 6d. Hence the symmetric solutions appear to be appropriate to out problem.

An isothermal model requires high thermal conductivity. Clearly at high altitudes with very low plasma density this assumptions no longer will be valid and the flow of the protons will be increasingly adiabatic. To check deviations of both models adiabatic flow will be discussed briefly in the following, too,

To account for finite thermal conductivity a polytropic law can be adopted:

$$\frac{P}{\varrho^\alpha}=\text{const}=\frac{P_0}{\varrho_0^\alpha} \tag{16}$$

(the index 0 indicating any fixed point, with $\alpha=1$ for isothermal and $\alpha=5/3$ for adiabatic conditions). In a realistic case α should vary along the field line. But as we

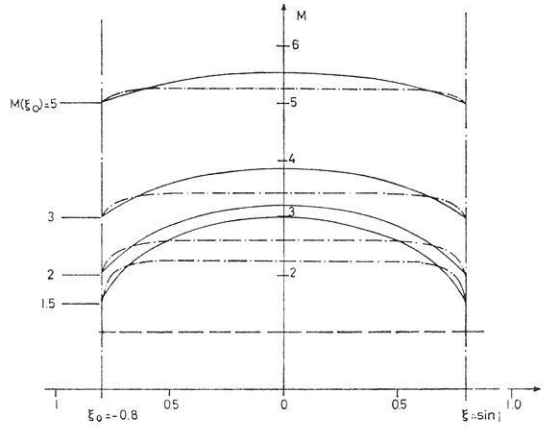

Fig. 7. Comparison of isothermal (———) and adiabatic (-·-·-) supersonic proton flow along closed field lines for H = 0.5

only intend to compare isothermal and adiabatic flow we assume it to be constant. Eq. (2) then can be integrated again to yield:

$$\frac{1}{2}(U^2 - U_0^2) + \left(\frac{2P_0}{\varrho_0}\right)\frac{\alpha}{\alpha - 1}\left[\left(\frac{U_0 A_0}{UA}\right)^{\alpha-1} - 1\right] + \varphi - \varphi_0 = 0 \qquad (17)$$

This corresponds to the integrals for the solar wind problem (Parker, 1963).

The speed of sound in the proton-electron plasma is determined by $c^2 = \partial P/\partial \varrho$ with $P = P_e + P_i$ and varies with height in the polytropic case according to the temperature variation. Accordingly the proton Machnumber should be defined by $M = U/c$. However, for easy comparison of isothermal and adiabatic conditions we introduce a formal proton Machnumber by $M = U/c_0$ where c_0 represents the isothermal speed of sound at the fixed point s_0 with $c_0^2 = 2P_0/\varrho_0$. In analogy to Eq. (14) the proton velocity distribution (17) then reads for the H^+-Mach-number:

$$\frac{1}{2}(M^2 - M_0^2) - \frac{H}{1 - \xi_0^2} - \frac{H}{1 - \xi^2} + \frac{\alpha}{\alpha - 1}\left[\left(\frac{M_0}{M}\,F(\xi^2)\right)^{\alpha-1} - 1\right] = 0 \qquad (18)$$

with

$$F(\xi^2) = \frac{(1 - \xi_0^2)^3}{\sqrt{1 + 3\xi_0^2}} \Big/ \frac{(1 - \xi^2)^3}{\sqrt{1 + 3\xi^2}} \qquad (19)$$

A complete solution pattern of (18) shall not be described here. Choosing H = 0.5 according to (15) and starting with supersonic velocities of $M(\xi_0) = 1.5$, 2.0, 3.0 and 5.0 at $\xi_0 = -0.8$ which corresponds to an altitude of 5100 km for $L = 5$ the velocity distribution along the field line up to the conjugate point is plotted in Fig. 7 both for isothermal and adiabatic flow (solid and dashed-dotted lines). Both models show a symmetric distribution with respect to the magnetic equator. For adiabatic conditions the protons are initially accelerated more rapidly than in the isothermal case, but soon

the H^+-velocity remains essentially constant, while further acceleration to a higher equatorial velocity occurs for isothermal conditions since more energy is available then. The essential features are not touched, however, and therefore from the consideration of the magnetospheric part of the flow it is concluded that the polar wind runs down into the conjugate nighttime ionosphere with the same particle density and mean velocity as produced by the daytime ionosphere. Hence the boundary conditions for the discussion of the winter nighttime ionosphere are characterized by an influx of supersonic plasma of some $10^8 cm^{-2} sec^{-1}$ with a mean velocity of 10—12 km/sec as provided by the illuminated side.

V. Supersonic Influx of Plasma into the Nighttime Ionosphere

As mentioned above diffusive influx of H^+-plasma of the order of $10^8 cm^{-2} sec^{-1}$ from the protonosphere is sufficient to maintain equilibrium F-layer densities of $10^5 cm^{-3}$ by charge exchange $H^+ + O \rightarrow O^+ + H$. In this section we discuss the question how the nighttime ionosphere is affected by a supersonic polar wind influx or vice versa for stationary conditions.

The principle structure of the hydrodynamic equations describing ionospheric processes is the same for daytime and nighttime. A critical solution also exists for supersonic influx where the speed of sound can be passed smoothly. (It should be pointed out that in contrast to daytime conditions, the nighttime critical solution does not represent a stable physical process, since this would require distinct boundary conditions for the incoming plasma. Any departure from these boundary values results in a departure from the critical solution. But if the particle density and mean velocity of the polar wind arriving at the nighttime ionosphere were close to the boundary values of the critical solution one should expect a weak stationary shock situated near the critical height.) One essential difference between outward and inward supersonic flow can be seen immediately from comparing the contributions of the various terms on the right hand side of Eq. (2). Assuming constant proton temperature Eq. (20) shows the sign of the different contributions for outward and inward flow.

$$\frac{1}{M}\frac{\partial M}{\partial s}(M^2-1) = \begin{array}{lll} & \text{out} & \text{in} \\ 1)\ \dfrac{\boldsymbol{\rho}\cdot\mathbf{s}}{c^2} & < 0 & < 0 \\ 2)\ +\dfrac{1}{A}\dfrac{\partial A}{\partial s} & > 0 & > 0 \\ 3)\ -\dfrac{1}{c^2}\displaystyle\sum_k \nu_k (U - U_k) & < 0 & > 0 \\ 4)\ -\dfrac{1}{\Phi}\dfrac{\partial \Phi}{\partial s} & < 0 & < 0 \\ 5)\ -\dfrac{T_e}{T_i}\dfrac{1}{n_e}\dfrac{\partial n_e}{\partial s} & > 0 & > 0 \\ 6)\ -q\dfrac{M^2 A}{\Phi} & < 0 & > 0 \end{array} \qquad (20)$$

Table 3

mod.	$\Phi(H^+)_{1000}$	h_{crit}	$v(H^+)_{3000}$	$M(H^+)_{3000}$	h_∞
$n(H)_{CIRA}$ $T_e = T_i = 1500$ K	$-3.49 \cdot 10^7$	385	17.2	4.90	1720
$10 \cdot n(H)_{CIRA}$ $T_e = T_i = 1500$ K	$-1.13 \cdot 10^7$	426	17.7	5.03	1670
$n(H)_{CIRA}$ $T_e = T_i = 3000$ K	$-1.54 \cdot 10^8$	383	27.9	5.61	5210
	[$cm^{-2} sec^{-1}$]	[km]	[km/sec]		[km]

CIRA = CIRA, Mod. 5, $t = 0$

The H^+-critical point is determined by vanishing of the right hand side of Eq. (20) for $M = 1$. The most important contributions arise from term 3), 4), and 5). The collision term 3) (with the $H^+ - O^+$-collisions most effective above 500 km) is < 0 (> 0) for $U > 0$ ($U < 0$). The polarization field 5) points to greater heights in both cases. The relative H^+-flux gradient $\frac{1}{\Phi}\frac{\partial \Phi}{\partial s}$ also acts in the same sense for outward and inward motion. While an outward directed proton flux ($\Phi > 0$) is built up at the expense of an O^+-flux $\left(\frac{\partial \Phi}{\partial s} > 0\right)$ for daytime conditions an inward H^+-flux ($\Phi < 0$) is converted into an O^+-flux $\left(\frac{\partial \Phi}{\partial s} < 0\right)$ in our nighttime model. The daytime critical point essentially results from a balance of the H^+-O^+-friction by the polarization field at greater heights where Φ is already nearly constant. In contrast to that the nighttime critical point must be shifted to rather low heights where chemical reactions are rapid and the relative flux gradient contribution can balance both friction and the electric field. According to the low critical height one also expects high transport speeds of the inward proton flux required by the nighttime critical solution so that supersonic flow down to the critical point is possible.

Corresponding to these considerations Table 3 lists numerical results of the nighttime critical solutions for three models with different ion temperatures and neutral hydrogen densities. The ion density and proton velocity distributions are plotted in Fig. 8 and 9.

The boundary values for the proton fluxes range from 10^7 to 10^8 cm^{-2} sec^{-1} thus maintaining equilibrium F-layer densities of only $4 \cdot 10^3$ to $5 \cdot 10^4$ cm^{-3} (Fig. 8). The critical point is located at about 400 km as compared with 2000 to 5000 km for the daytime solutions. Continuous deceleration to subsonic speed is only possible with initial velocities (at 3000 km height) as high as 17—18 km/sec for the 1500 K model and 28 km/sec for the 3000 K model. This is equivalent to Machnumbers of about 5 for all cases. The proton velocity decreases rather slowly towards lower heights. Only near the critical point a rapid deceleration to very low velocities is effective (Fig. 9).

In Sect. III results of the daytime models indicated that the sunlit polar ionosphere

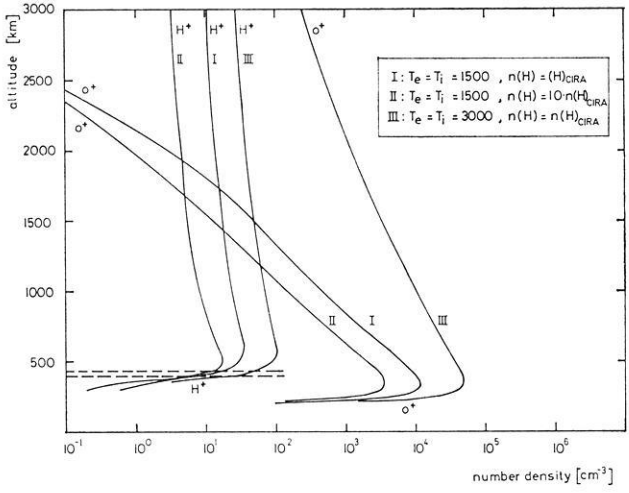

Fig. 8. Ion density profiles for the nighttime critical solution for three different models

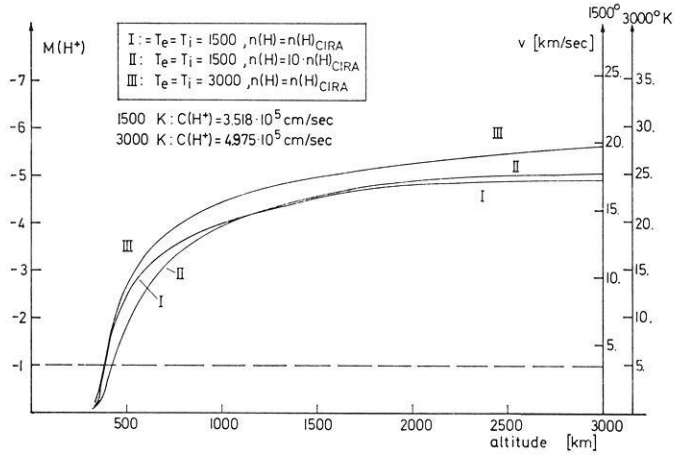

Fig. 9. Proton velocity profiles for the nighttime critical solution for three different models. The critical point lies very low as compared to daytime conditions

yields polar wind fluxes with Machnumbers not exceeding 4 at high altitudes. Since the free flow in the magnetosphere is symmetric with respect to the equator (Section IV), this implies an upper limit for the Machnumber of the plasma flow arriving at the nighttime ionosphere that is considerably less than required by the critical solutions. Consequently the realistic polar wind has to be decelerated discontinously to subsonic speed and shock waves have to be built up.

Concerning the problem of maintaining high latitude nighttime *F*-layers by a supersonic plasma influx the essential question is whether these shock waves can be stationary. The mass flux is only conserved in a coordinate system where the shock

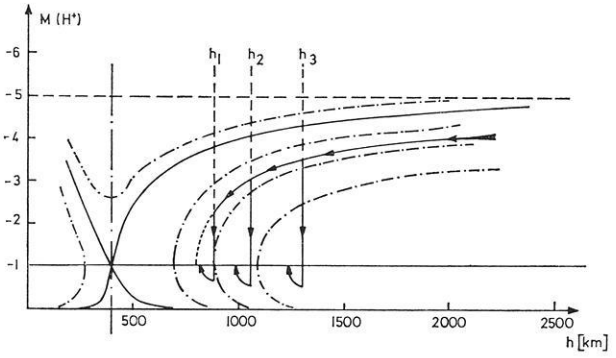

Fig. 10. Schematic solution pattern for nighttime inward plasma flow. A polar wind arriving with a Mach number of 4 cannot be decelerated strongly enough in a stationary shock wave to follow a physically reasonable subsonic solution

wave is at rest. Hence a non-stationary shock wave causes a reduction of the proton flux in a fixed coordinate system. As the equilibrium F-layer densities are proportional to the inward fluxes (e.g. Rishbeth, 1963) a non-stationary shock wave implies a reduction of the equilibrium layer.

Fig. 10 serves to illustrate that the formation of a stationary shock wave is not possible since it would decelerate the polar wind only insufficiently. A schematic solution pattern for the hydrogen ion velocities is shown. The critical solution agrees with the results plotted in Fig. 9 and accordingly has to start with a Mach number of 5 at great heights. We choose the case of a polar wind arriving with a Machnumber of 4 which proved to be an upper limit for the H^+-velocity from our dayside considerations. (Clearly the following conclusions hold as well for lower velocities than $M = 4$.) It would follow the velocity path indicated by the arrow. We try to locate a stationary shock at the heights h_1, h_2, or h_3. The compression of the H^+-plasma is, however, limited to a factor of about 4 according to the Rankine-Hugoniot-relations. Therefore, the hydrogen ions can be decelerated to a Machnumber of 0.5 to 0.6 in the shock wave and fail to reach a subsonic solution which can satisfy the boundary conditions at lower heights. They would be accelerated rather rapidly to sonic speed again. Hence the H^+-plasma must be decelerated more effectively than can be achieved by a stationary shock wave. Nonstationary shock waves will be set up propagating into the supersonic region. The limitation of the plasma discontinuity to a density ratio of 4 results from converting flow energy into thermal energy. The corresponding pressure increase prevents a stronger compression. It should be noted, however, that nonstationary shock waves are required even for an isothermal shock. (Clearly we cannot assume isothermal shocks to be set up by the incoming polar wind as the energy transfer to the oxygen ions is not effective enough. The ratio of the collision frequency for momentum transfer to the collision frequency for energy transfer is $(m(H^+) + m(O^+))/2m(H^+) = 8.5$ for the H^+-O^+-collisions (Eq. (6)). Hence the energy exchange between both ion species will not be significant within the shock that is within a few mean free paths. Nevertheless we want to consider isothermal shock conditions as an extreme case allowing maximum compression to support our conclusion that non-stationary shock waves have to originate.) Con-

servation of mass and momentum flux (the energy flux is not conserved in this case) with zero shock velocity yields $M^+ = 1/M^-$ where M^+, M^- denote the respective Machnumbers at the post- and pre-shock side (viewed from the supersonic region). As $|M^-| \leqslant 4$ one gets $|M^+| \geqslant 0.25$. This is still much to fast for reaching a physically reasonable subsonic solution in the velocity pattern of Fig. 10.

In order to extend our time-independent calculations to non-stationary shock waves we make the assumption that the only temporal dependence originates from the upward motion of the shock wave. The ion density distribution can then be described by

$$n(h, t) = n^+(h) + (n^-(h) - n^+(h)) \cdot \mathrm{H}(h - h_0) \tag{25}$$

with the step function $\mathrm{H}(x - x_0)$ defined by

$$\begin{aligned} \mathrm{H}(x - x_0) &= 0 \text{ for } x < x_0 \\ \mathrm{H}(x - x_0) &= 1 \text{ for } x > x_0 \end{aligned} \tag{26}$$

$n^+(h)$ represents a time independent solution describing the subsonic region, $n^-(h)$ the corresponding solution for the supersonic regime. h_0 denotes the momentary position of the shock wave at time t_0 and is given by

$$h_0 = h^* + \int_{t^*}^{t_0} u \, dt \tag{27}$$

(u = shock wave velocity), where h^* stands for the height where the shock wave at time t^* originally arises.

In the following numerical results of this model will be presented. We choose a supersonic proton influx of $3 \cdot 10^8 \mathrm{cm}^{-2}\mathrm{sec}^{-1}$ with $T(\mathrm{H}^+)_{3000} = 1500$ K and $M(\mathrm{H}^+)_{3000} = -4$ as boundary values at 3000 km height. The proton temperature varies, as before, with height in accordance to Eq. (3). The oxygen ions and the electrons are assumed to be isothermal with $T(\mathrm{O}^+) = T_e = 1500$ K. The O^+-flux at 3000 km is taken to be zero. Hence the O^+-density at this height and the shock velocity as a function of position have to be determined from the boundary conditions at lower heights. These boundary conditions require the vanishing of both H^+- and O^+-flux at low altitudes, and $n(\mathrm{O}^+)_{3000}$ and the shock velocity have to be adjusted until a solution is obtained having the proper characteristics. If $n(\mathrm{O}^+)_{3000}$ is chosen too low the oxygen ions follow a physically unreasonable solution and the H^+-ions still remain supersonic. With sufficiently high $n(\mathrm{O}^+)_{3000}$ the hydrogen ions reach $M(\mathrm{H}^+) = -1$ at a height h^* as sketched in Fig. 10. Now one can choose several heights h_i above h^* and adjust the shock wave velocity $u(h_i)$ so as to satisfy the boundary condition for the proton flux at low heights ($\Phi(\mathrm{H}^+) \to 0$ for $h \to 0$). After this has been achieved the O^+-flux normally will not vanish simultaneously at low altitudes. Then $n(\mathrm{O}^+)_{3000}$ must be appropriately corrected and the whole procedure has to be repeated until $n(\mathrm{O}^+)_{3000}$ is sufficiently accurate.

(It should be pointed out that the numerical results derived in that way are not fully consistent with our assumption of time-independence at both sides of the shock wave. As may be seen from Fig. 11 and 13 different locations of the shock would

cause slightly different H^+-density profiles in the subsonic region and partly even affect the O^+-density distribution too. For a non-stationary shock wave a higher shock location, however, simply corresponds to a view at the same situation at some later moment. This behaviour thus clearly reveals an explicit time-dependence which has been excluded before. But as it seems to be very difficult to perform time-dependent polar wind calculations this discrepancy must be accepted here).

Fig. 11 shows the results for an equilibrium F-layer maintained by a polar wind influx with the characteristics listed above. The oxygen and hydrogen ion densities are plotted in Fig. 11a for three different positions of the shock wave equivalent to three successive snapshots. The shock originates at a height of about 1100 km and runs upward filling the flux tube continuously with denser and hot hydrogen plasma. The proton flux is reduced by the shock wave to $6.2 \cdot 10^7 \mathrm{cm}^{-2}\mathrm{sec}^{-1}$ that is to one fifth of its original value and can therefore maintain F-layer densities of only $2.1 \cdot 10^4$ cm^{-3}. The proton velocity is shown in Fig. 11b. As already discussed the protons have to be decelerated within the shock to very low velocities. The numerical results indicate that the post-shock proton Mach-number has to be about 0.1 in order to reach a physically reasonable subsonic solution. The shock velocity u_s which turns out to be $\sim$5.5 km/sec is plotted in Fig. 11c. The protons are heated to a temperature of nearly 10^4K (Fig. 11d). The proton temperature then remains essentially constant down to about 800 km from which height the energy transfer to the oxygen ions becomes effective. The protons thereby are cooled to the background temperature within a region of less than 200 km.

Compared with the very low equilibrium F-layer density derived above experimental research of high latitude ionospheres yields a quite different picture (a synopsis of trans-polar plasma is given for example by Thomas and Andrews (1969)). With the exception of the polar cavity which is on open field lines the polar F-regions show a base level of the order of $10^5\mathrm{cm}^{-3}$ below which the maximum density does not fall even during winter night (Rishbeth, 1968).

Hence we can change our point of view and instead of calculating equilibrium F-layers consider a polar wind running into a nighttime ionosphere with an O^+-density distribution as observed. Results are shown in Fig. 12. The O^+-density profile was chosen somewhat arbitrarily as the equilibrium layer with $T(O^+) = 1500$ K provided by a diffusive proton influx of $3 \cdot 10^8 \mathrm{cm}^{-2}\mathrm{sec}^{-1}$ which just creates a maximum density of $10^5\mathrm{cm}^{-3}$. The resulting proton velocity and temperature are very similar to the previous ones. Again non-stationary shock waves are formed reducing the initial polar wind flux to a post-shock flux of $5.4 \cdot 10^7 \mathrm{cm}^{-2}\mathrm{sec}^{-1}$. The shock velocity of about 6 km/sec turns out slightly higher.

Both examples therefore indicate that only a small portion of a supersonic proton flux with the above characteristics can advance to F-region heights and that such an influx will not influence the polar F-region strongly. Fig. 13 and 14 demonstrate that this conclusion still holds for isothermal flow conditions and an isothermal shock wave which allows a higher compression. In spite of the much lower shock wave velocities of about 1.5 km/sec (for the higher shock wave positions) the post-shock fluxes are again very low. The discontinuity of the mass flux in a fixed coordinate system is given by $\varrho^+ U^+ - \varrho^- U^- = u_s(\varrho^+ - \varrho^-)$. The lower shock wave velocity u_s is balanced in this case by the higher compression by the isothermal shock wave. In the calculation of an equilibrium layer the post-shock flux is $4.4 \cdot 10^7 \mathrm{cm}^{-2}\mathrm{sec}^{-1}$

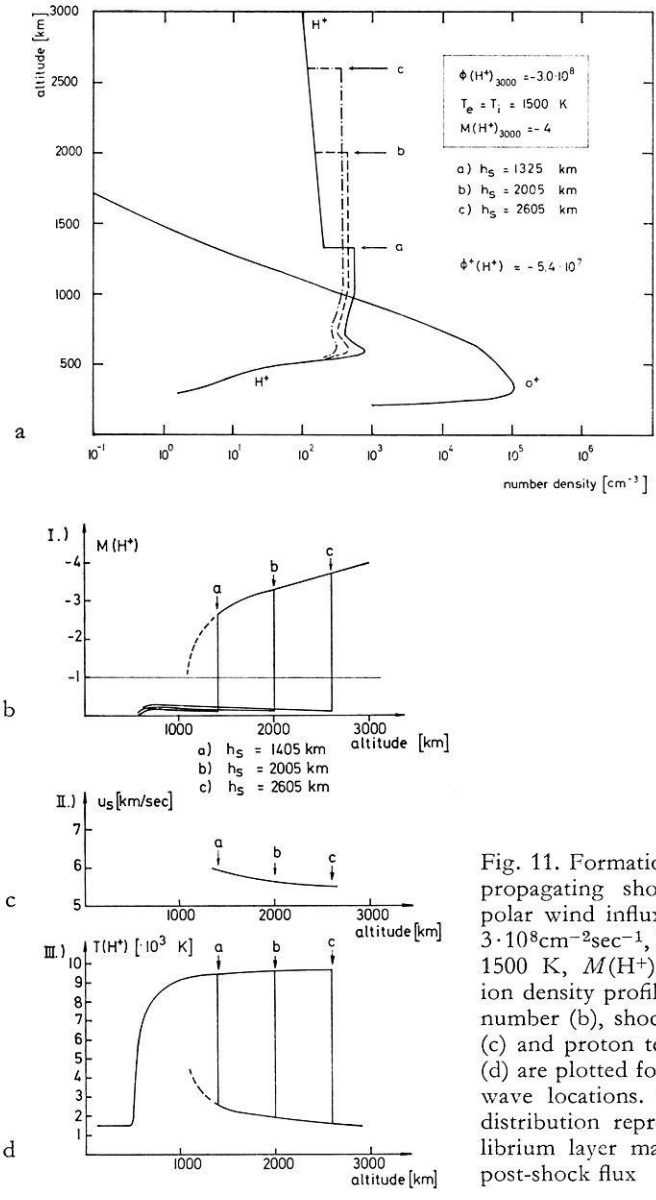

Fig. 11. Formation of an upward propagating shock wave by a polar wind influx of $3 \cdot 10^8 cm^{-2} sec^{-1}$, $T(H^+)_{3000} =$ 1500 K, $M(H^+)_{3000} = -4$. The ion density profiles (a), H^+-Mach number (b), shock wave velocity (c) and proton temperature (d) are plotted for different shock wave locations. The O^+-density distribution represents the equilibrium layer maintained by the post-shock flux

maintaining a maximum density of $1.8 \cdot 10^4 cm^{-3}$ similarly to the results shown in Fig. 11. The model with a fixed O^+-density distribution yields a very high reduction of the inward flux, namely to $3.4 \cdot 10^6 cm^{-2} sec^{-1}$, i.e. to one twentieth of the initial value.

The path of the protons between both conjugate ionospheres along a dipole field line with an L-value of 5 amounts to 75000 km. If the shock wave were travelling with a constant velocity of 5 km/sec from the nighttime to the daytime ionosphere which is emitting polar wind fluxes the supersonic flow could only survive for 4.2 h.

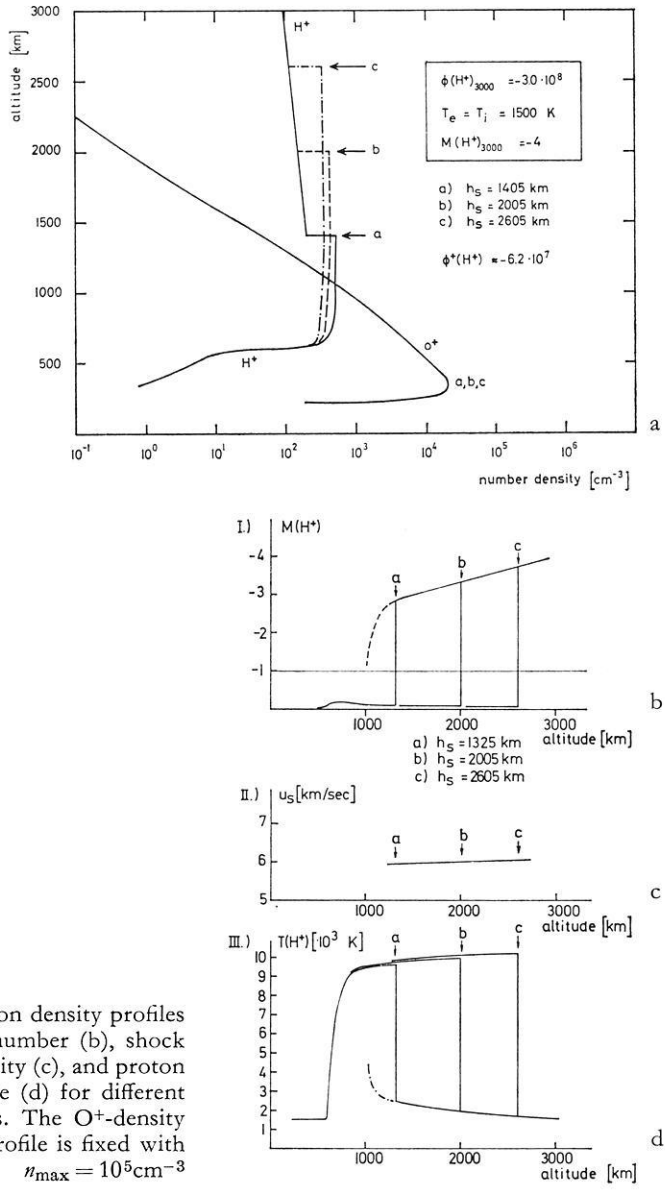

Fig. 12. Ion density profiles (a), H^+-Mach number (b), shock wave velocity (c), and proton temperature (d) for different shock locations. The O^+-density profile is fixed with $n_{max} = 10^5 cm^{-3}$

The method employed in this paper to determine the shock wave velocity, however, cannot be extended to arbitrary altitudes. It is based on performing stationary calculations implying that the protons 'know' about the boundary conditions at low altitudes at the nighttime side. Disturbances and the corresponding information are transferred in a plasma with speed of sound. If the propagation time of this information is of the same order as the time scale of temporal variations the assumption of stationary conditions no longer will be justified and the two regions essentially will be decoupled. That is, at a height of about 20000 km at most equivalent to a propaga-

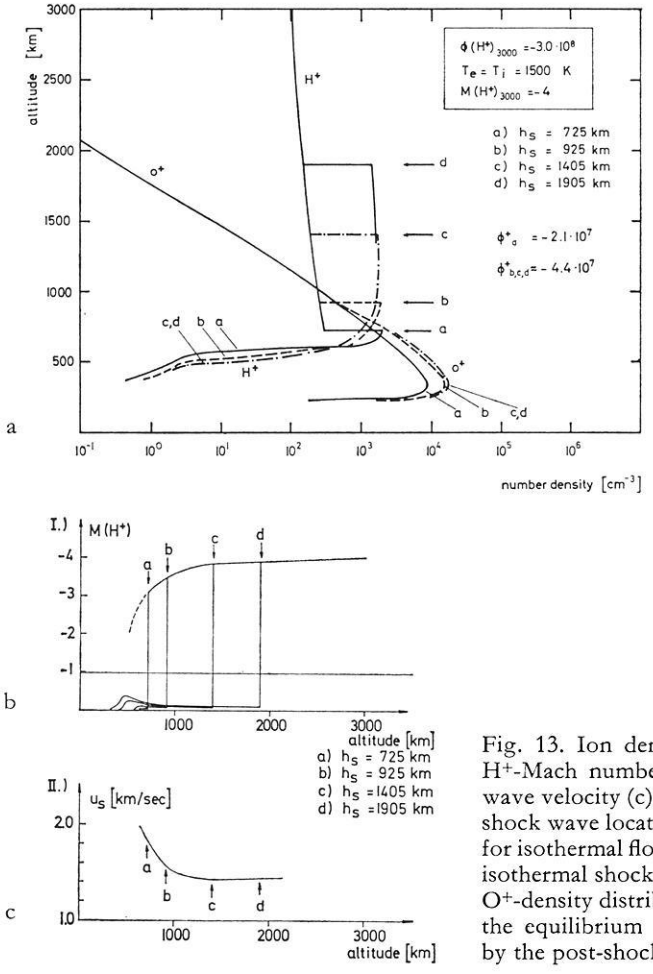

Fig. 13. Ion density profiles (a), H^+-Mach number (b) and shock wave velocity (c) for different shock wave locations computed for isothermal flow conditions and isothermal shock wave. The O^+-density distribution represents the equilibrium layer maintained by the post-shock flux

tion time of the order of one hour our calculation of the shock wave velocity from the ionospheric boundary conditions will not be reasonable any longer. The shock velocity must be determined then from similar considerations as given by Banks *et al.* (1971) in their discussion of a symmetric geomagnetic configuration. Hence their conclusion that a polar wind on closed field lines would be switched off within 22 h for $L = 5$ and (bearing in mind the time scales of the convection cycle of polar flux tubes) can represent a rather steady phenomenon also for closed flux tubes is not affected by the results described in this paper.

VI. Conclusions

The coupling of the winter nighttime ionosphere to the summer daytime ionosphere at high latitudes by a polar wind running along closed field lines has been discussed in this paper in a stationary model. It has been shown that shock waves

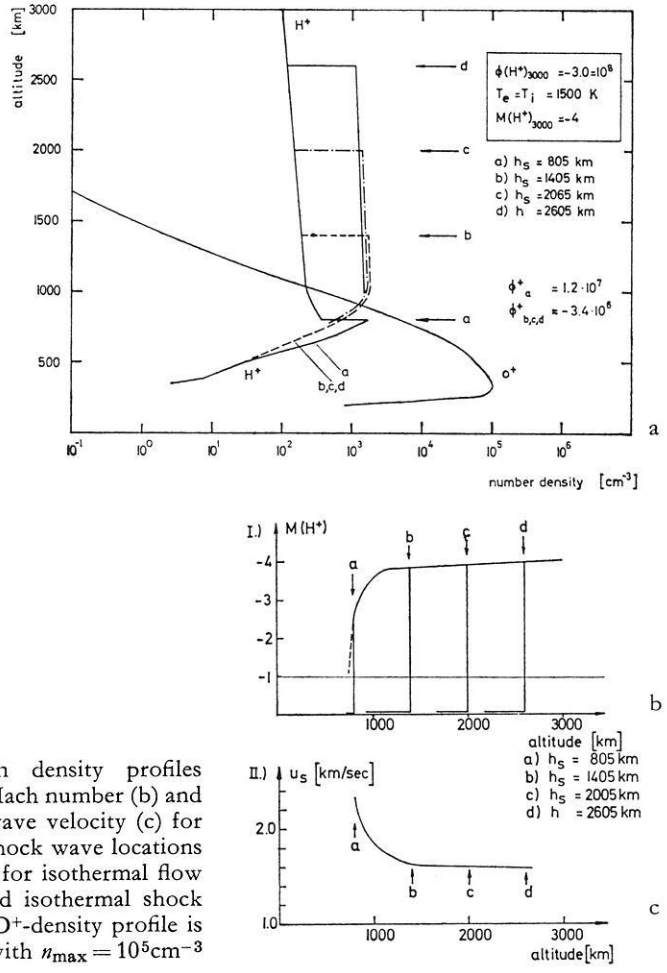

Fig. 14. Ion density profiles (a), H^+-Mach number (b) and shock wave velocity (c) for different shock wave locations computed for isothermal flow conditions and isothermal shock wave. The O^+-density profile is fixed with $n_{max} = 10^5 cm^{-3}$

with upward velocities of about 5 km/sec would form above the dark ionosphere reducing the inward fluxes considerably. Consequently such a mechanism can only be of minor influence upon polar *F*-region behaviour. However, the ionization of a polar flux tube would be changed by the passage of the shock wave at higher altitudes. If a polar orbiting satellite were traversing such a shock front the change of the plasma parameters could be easily confused with a discontinuity parallel to the magnetic field. This discussion shall emphasize the possibility of horizontal discontinuities set up by supersonic plasma influx arising from the sunlit hemisphere.

There is growing evidence that the most effective ionization source for maintaining polar winter *F*-layers and causing UT-variations (e.g. Maehlum, 1968, 1969) is corpuscular radiation with low energy electrons (50 eV–1 keV) being most important for ionization. (Many aspects of polar ionospheres are for example summarized in G. Skovli, Ed.: The polar ionosphere and magnetospheric processes). Due to plasma convection this source of ionization can extend its influence to distances quite far from the region of energetic particle influx (like the dayside polar cusp).

Acknowledgement. The author is grateful to Dr. G. Haerendel for valuable discussions and helpful advice during the preparation of this paper.

References

Axford, X.I., Hines, C.O.: A unifying theory of high-latitude geophysical phenomena and geomagnetid storms. Can. J. Phys. *39*, 1433–1464, 1961

Banks, P.M., Holzer, T.E.: The polar wind. J. Geophys. Res. *73*, 6846–6854, 1968

Banks, P.M., Holzer, T.E.: High-latitude plasma transport: the polar wind. J. Geophys. Res. *74*, 6317–6332, 1969a

Banks, P.M., Holzer, T.E.: Features of plasma transport in the upper atmosphere. J. Geophys. Res. *74*, 6304–6316, 1969b

Banks, P.M.: Plasma transport in the topside ionosphere. In: The polar ionosphere and magnetospheric processes. G. Skovli, ed., pp. 193–208, New York: Gordon & Breach 1970

Banks, P.M., Nagy, A.F., Axford, W.I.: Dynamical behaviour of thermal protons in the mid-latitude ionosphere and magnetosphere. Planetary Space Sci. *19*, 1053–1067, 1971

Banks, P.M.: Dynamical behaviour of the polar topside ionosphere, presented at the NATO Advanced Study Institute on Magnetosphere-Ionosphere Interactions. Espedalen, Norway, 1971

Banks, P.M., Kockarts, G.: Aeronomy. New York: Academic Press 1973

Brace, L.H., Reddy, B.M., Mayr, H.G.: Global behaviour of the ionosphere at 1000 km altitude. J. Geophys. Res. *72*, 265–283, 1967

Brice, N.M.: Bulk motion of the magnetosphere. J. Geophys. Res. *72*, 5193–5211, 1967

Brinton, H.C., Grebowsy, J.M., Mayr, H.G.: Altitude variation of ion composition in the mid-latitude trough region: evidence for upward plasma flow. J. Geophys. Res. *76*, 3738–3745, 1971

Dungey, J.W.: Interplanetary magnetic field and the auroral zones. Phys. Rev. Letters *6*, 47–48, 1961

Dunkin, D.B., Fehsenfeld, F.C., Schmeltekopf, A.L., Ferguson, E.E.: Ion-molecule reaction studies from 300° to 600° K in a temperature-controlled afterglow system. J. Chem. Phys. *49*, 1365–1371, 1968

Evans, J.V.: Cause of the mid-latitude winter night increase in f_0F2. J. Geophys. Res. *70*, 4331–4345, 1965

Ferguson, E.E.: Ionospheric ion-molecule reaction rates. Rev. Geophys. *5*, 305, 1967

Geisler, J.E.: On the limiting daytime flux of ionization into the protonosphere. J. Geophys. Res. *72*, 81–85, 1967

Hanson, W.B., Patterson, T.N.L.: The maintenance of the nighttime *F*-layer. Planetary Space Sci. *12*, 979–997, 1964

Hoffman, J.X.: Ion composition measurements in the polar region from the Explorer 31 Satellite. Trans. Am. Geophys. Union *49*, 253, 1968

Hoffman, J.W.: Polar wind measurements. Trans. Am. Geophys. Union *4*, 301, 1971

Holzer, T.E., Banks, P.M.: Accidentally resonant charge exchange and ion momentum transfer. Planetary Space Sci. *17*, 1074–1077, 1969

Holzer, T.E.: Effects of plasma flow on density and velocity profiles in the polar ionosphere: In: The Polar Ionosphere and Magnetospheric Processes. G. Skovli, ed. pp. 209–223. New York: Gordon & Breach

Holzer, T.E., Fedder, J.A., Banks, P.M.: A comparison of kinetic and hydrodynamic models of an expanding ion-exosphere. J. Geophys. Res. *76*, 2453–2468, 1971

Holzer, T.E.: Interaction of the solar wind with the neutral component of the interstellar gas. J. Geophys. Res. *77*, 5407–5431, 1972

King, J.W., Kohl, H., Pratt, R.: The effect of atmospheric winds on the height of the *F*2-layer peak at middle and high latitudes. J. Atmospheric Terrest. Phys. *29*, 1529–1539, 1967

Kohl, H.: The possible effect of diffusion between magnetically conjugate points on the seasonal anomaly of the *F*-layer. In: Electron density profiles in ionosphere and exosphere. J. Frihagen, ed. pp. 231–238, North-Holland, Amsterdam: Publ. Co. 1966

K ohl, H., King, J.W., Eccles, D.: Some effects of neutral winds on the ionospheric *F*-layer. J. Atmospheric Terrest. Phys. *30*, 1733–1744, 1968
Maehlum, B.N.: Universal-time control of the low-energy electron fluxes in the polar regions. J. Geophys. Res. *73*, 3459–3468, 1968
Maehlum, B.N.: On the high-latitude, universal time controlled *F*-layer. J. Atmospheric Terrest. Phys. *31*, 531–538, 1969
Mayr, H.G., Brace, L.H., Dunham, G.S.: Ion composition and temperature in the topside ionosphere. J. Geophys. Res. *72*, 4391–4404, 1967
Mayr, H.G., Grebowsy, J.M., Taylor, H.A.: Study of the thermal plasma on closed field lines outside the plasmasphere. Planetary Space Sci. *18*, 1123–1135, 1970
Mitra, A.P.: A review of D-region processes in non-polar latitudes. J. Atmospheric Terrest. Phys. *30*, 1065–1114, 1968
Nagy, A.F., Bauer, P., Fontheim, E.G.: Nighttime cooling of the protonosphere. J. Geophys. Res. *73*, 6259–6274, 1968
Nishida, A.: Formation of a plasmapause, or magnetospheric plasma knee by the combined action of magnetospheric convection and plasma escape from the tail. J. Geophys. Res. *71*, 5669–5679, 1966
Park, C.G.: Whistler observations of the interchange of ionization between the ionosphere and the protonosphere. J. Geophys. Res. *75*, 4249–4260, 1970
Park, C.G., Banks, P.M.: Influence of thermal plasma flow on the mid-latitude nighttime F_2-layer: Effects of electric fields and neutral winds inside the plasmasphere. J. Geophys. Res. *79*, 4661–4668, 1974
Parker, E.N.: Interplanetary dynamical processes. New York: Wiley 1963
Rishbeth, H.: Further analogue studies of the ionospheric *F*-layer. Proc. Phys. Soc. (London) *81*, 65–77, 1963
Rishbeth, H.: On explaining the behaviour of the ionospheric *F*-region. Rev. Geophys. *6*, 33–71, 1968
Rishbeth, H.: The polar *F*-region. In: The polar ionosphere and magnetospheric processes. G. Skovli, ed. pp. 175–192. New York: Gordon & Breach 1970
Rösler, G.: Plasmaüberschallströmung zwischen magnetisch konjugierten Ionosphären hoher Breiten. MPI-PAE/Extraterr. 97, 1974
Rüster, R.: The relative effects of electric fields and atmospheric composition changes on the electron concentration in the mid-latitude *F*-layer. J. Atmospheric Terrest. Phys. *33*, 275–280, 1971
Skovli, G., ed.: The polar ionosphere and magnetospheric processes. New York: Gordon & Breach 1970
Stubbe, P.: Temperature dependence of the rate constants for the reactions $O^+ + O_2 \rightarrow O_2^+ + O$ and $O^+ + N_2 \rightarrow NO^+ + N$. Planetary Space Sci. *17*, 1221–1231, 1969
Stubbe, P., Chandra, S.: The effects of electric fields on the *F*-region behaviour as compared with neutral wind effects. J. Atmospheric Terrest. Phys. *32*, 1909–1919, 1970
Tanenbaum, B.S.: Transport equations for a gas mixture. Phys. Fluids *8*, 683–686, 1965
Thomas, J.O., Andrews, M.K.: The trans-polar exospheric plasma, 3: a unified picture. Planetary Space Sci. *17*, 433–446, 1969
Thomas, L.: The importance of photoionization in the production of the daytime *F*-region at high latitudes during winter. Planetary Space Sci. *14*, 891–899, 1966
Torr, D.G., Torr, M.R.: A theoretical investigation of corpuscular radiation effects on the *F*-region of the ionosphere. J. Atmospheric Terrest. Phys. *32*, 15–34, 1970
Yonezawa, T.: Maintenance of ionization in the nighttime F_2-region. Space Res. *5*, 49–60, 1965.

Dr. G. Rösler
Max-Planck-Institut für Physik und Astrophysik
Institut für extraterrestrische Physik
D-8046 Garching bei München
Federal Republic of Germany